Journal of Power Sources 195 (2010) 4727–4730

Contents lists available at ScienceDirect

Journal of Power Sources

journal homepage: www.elsevier.com/locate/jpowsour

Short communication

Fabrication and performance of a proton-conducting solid oxide fuel cell based on a thin $BaZr_{0.8}Y_{0.2}O_{3-\delta}$ electrolyte membrane

Wenping Sun, Litao Yan, Zhen Shi, Zhiwen Zhu, Wei Liu*

CAS Key Laboratory of Materials for Energy Conversion, Department of Materials Science and Engineering, University of Science and Technology of China (USTC), Hefei, 230026, PR China

ARTICLE INFO

Article history:
Received 11 January 2010
Received in revised form 4 February 2010
Accepted 4 February 2010
Available online 10 February 2010

Keywords:
Proton-conducting solid oxide fuel cells
Yttrium-doped barium zirconate
Membrane
Performance

ABSTRACT

A dense $BaZr_{0.8}Y_{0.2}O_{3-\delta}$ (BZY) proton-conducting electrolyte membrane is successfully fabricated on a NiO–$BaZr_{0.1}Ce_{0.7}Y_{0.2}O_{3-\delta}$ (NiO–BZCY) anode substrate by a co-pressing process after co-firing at 1400 °C. BZY powders are synthesized via a citric acid–nitrate gel combustion process after calcination at 1100 °C. The SEM results reveal that the BZY membrane is crack-free, very dense, and 20 μm thick. A single cell with $Sm_{0.5}Sr_{0.5}CoO_{3-\delta}$–$Ce_{0.8}Sm_{0.2}O_{2-\delta}$ (SSC–SDC) as the cathode is assembled and tested with wet hydrogen (2% H_2O) as the fuel and static air as the oxidant. The open circuit voltages (OCVs) are 0.953, 0.987, 1.014, and 1.039 V at 700, 650, 600, and 550 °C, respectively. A maximum power density of 170 mW cm^{-2} is obtained at 700 °C. Resistances of the testing cell are investigated under open circuit conditions at different operating temperatures by impedance spectroscopy.

1. Introduction

Perovskites based on $BaCeO_3$ and $BaZrO_3$ doped with Y_2O_3 or lanthanide oxides have been widely investigated as electrolytes for proton-conducting solid oxide fuel cells (H-SOFCs). Acceptor doped $BaCeO_3$-based oxides are the current material of choice for proton conductors, and consequently have been investigated extensively [1–4]. However, they have poor chemical stability against H_2O and CO_2, which limits their practical applications [5,6]. In comparison, acceptor doped $BaZrO_3$ exhibits good chemical stability, and Y_2O_3-doped $BaZrO_3$ (BZY) has been investigated in detail by several research groups [7–10]. The reported proton conductivities of BZY vary between studies, and this might be correlated with the process by which they were synthesized. The proton conductivity of BZY single crystal is of the same order of magnitude as that of yttrium-doped barium cerate (BCY) [11]. However, $BaZrO_3$ has a very poor sintering ability and can only be sintered at as high as 1700 °C [12,13]. This high sintering temperature leads to barium evaporation which lowers conductivity, and makes it difficult to choose substrate materials with sufficient porosity after co-sintering. Fabrication of a dense BZY electrolyte membrane on a porous anode substrate is a considerable challenge, and this prevents the fabrication of H-SOFC based on BZY. To the best of our knowledge, an anode-supported BZY membrane has not been fabricated yet.

In this study, we employed a co-pressing and co-firing method to fabricate a BZY membrane on a NiO–$BaZr_{0.1}Ce_{0.7}Y_{0.2}O_{3-\delta}$ (NiO–BZCY) anode substrate at a relatively low sintering temperature of 1400 °C. The BZY powders were synthesized via a citric acid–nitrate gel combustion process after being calcined at 1100 °C. The electrochemical performance of a BZY-based single cell was also investigated.

2. Experimental

2.1. Powder synthesis and cell fabrication

BZY powders were synthesized via a citric acid–nitrate gel combustion process [14]. First, Y_2O_3 was dissolved in HNO_3, and then $Zr(NO_3)_4{\cdot}5H_2O$ was added to the solution with stirring and heating on a hot plate. After the solution became clear, $Ba(CH_3COO)_2$ was then added. Citric acid was added in a 1:1.5 metal ions: citric acid molar ratio and the pH value adjusted to about 7 with ammonia. The solution was heated and stirred continuously at about 70 °C until gelling. The gel was then moved to an evaporation pan heated on a hot plate. Gel ignition and combustion then occurred, yielding the as-prepared powders. Then the as-prepared powders were calcined at 1100 °C for 5 h in air to form a pure perovskite phase $BaZr_{0.8}Y_{0.2}O_{3-\delta}$. The NiO–$BaZr_{0.1}Ce_{0.7}Y_{0.2}O_{3-\delta}$ (NiO–BZCY) composite powders (weigh ratio of 3:2) for the anode substrate were also prepared by the citric acid–nitrate gel combustion process described above. The composite anode powders were calcined at 1000 °C for 3 h to eliminate any nickel.

* Corresponding author. Tel.: +86 551 3606929; fax: +86 551 3602586.
E-mail address: wliu@ustc.edu.cn (W. Liu).

0378-7753/$ – see front matter © 2010 Elsevier B.V. All rights reserved.
doi:10.1016/j.jpowsour.2010.02.012

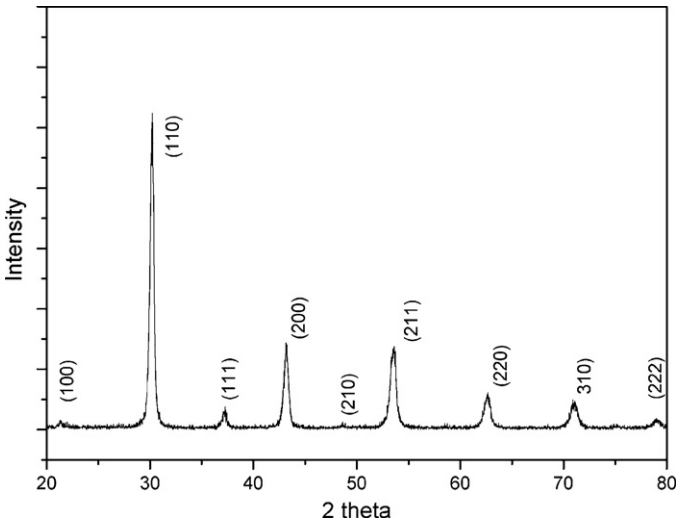

Fig. 1. XRD pattern of the BZY powder calcined at 1100 °C for 5 h.

The green anode-supported half-cells were fabricated by a co-pressing method. First, the NiO–BZCY powders were pressed in a stainless steel module to form an anode substrate with a flat surface and a certain mechanical strength. Then, the loose high-activity BZY powders were added and evenly distributed onto the substrates with a flat sheet of metal. The BZY layer was then pressed together with the anode substrate. The thickness of the BZY membrane could be controlled by varying the amount of powder used. Finally, the green half-cells were co-fired at 1400 °C for 10 h. It should be noted that no pore-creating materials such as starch were added to the anode substrate. $Sm_{0.5}Sr_{0.5}CoO_{3-\delta}$–$Ce_{0.8}Sm_{0.2}O_{2-\delta}$ (SSC–SDC, weigh ratio 3:2) composite cathode slurry was brush painted onto the BZY electrolyte membrane, and sintered at 1000 °C for 3 h in air to form a porous cathode layer. Ag paste was applied to the cathode as a current collector.

2.2. Characterization of phase composition and microstructures of powders and cell components

Phase structures of the BZY powder and membrane were identified by X-ray diffraction (XRD) analysis on a Philips PW 1730 diffractometer using CuKα radiation. The microstructures of the BZY powders and membrane, and the tested cell were examined by SEM (JEOL JSM-6700F).

2.3. Electrochemical measurement of single cells

We constructed a cell-testing system and used it to test single cells from 550 to 700 °C with humidified hydrogen (2% H_2O) as the fuel and static air as the oxidant, respectively. The flow rate of the fuel gas was about 30 mL min^{-1}. The cell performance was measured with a DC Electronic Load (ITech Electronics model IT8511). Resistances of the cell under open circuit conditions were measured with an impedance analyzer (CHI604B, Shanghai Chenhua). A 5 mV a.c. signal was applied and the frequency was swept from 100 kHz to 0.1 Hz.

3. Results and discussion

Fig. 1 shows the XRD pattern of the BZY powder after it was calcined at 1100 °C for 5 h. The lattice parameter and the cell volume of BZY were calculated to be $a = 4.1989(5)$ Å and $V = 74.03$ Å^3, respectively. The SEM image of the BZY powder (Fig. 2) shows it is coral-like and loose, which is typical for powders prepared via a gel combustion process. This allows it to be very easily crushed to fine nanometer scale powders.

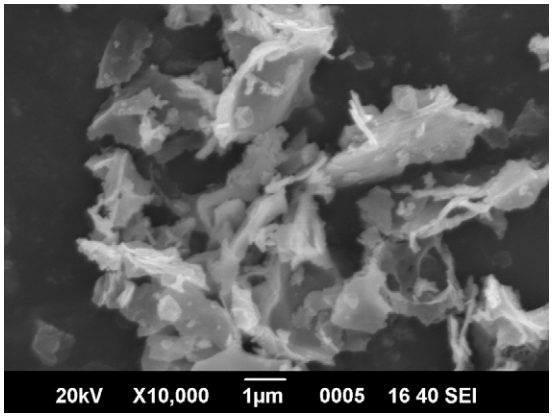

Fig. 2. SEM image of the BZY powder.

Fig. 3 presents the XRD pattern of the nominal BZY electrolyte membrane supported on a NiO–BZCY ceramic substrate after co-sintering at 1400 °C for 10 h. Except for some minor peaks of yttrium stabilized zirconia (YSZ), which was introduced by evaporation of some barium at high temperatures [15], only peaks corresponding to cubic perovskite BZY were observed in the XRD pattern. Therefore, a lower fabrication temperature is required in order to obtain a pure BZY membrane.

SEM images of the BZY electrolyte membrane surface morphology were obtained before (Fig. 4(a)) and after testing (Fig. 4(b)), and of the cross-section after testing (Fig. 4(c)). It is clear that the electrolyte membrane is very dense, apart from some closed pores in the cross-section. The grain size is also very small, less than 1 μm, which might result in a large grain boundary resistance and hence induce low membrane conductivity [16]. Fig. 4(d–f) shows the SEM images of cross-sections of the tested cell. Fig. 4(d and e) shows that the BZY membrane is about 20 μm thick and that adhesion of the BZY membrane to the Ni–BZCY anode substrate seems to be excellent. This dense and crack-free membrane confirms that combined co-pressing and co-firing at 1400 °C is a feasible method for the fabrication of anode-supported BZY electrolyte membrane. However, since no pore-creating materials such as starch were added to the anode substrate, the porosity of the anode is very low (Fig. 4(f)). This

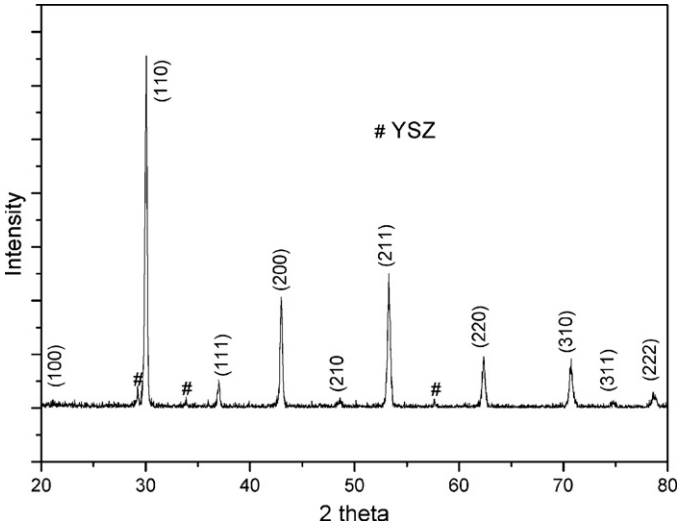

Fig. 3. XRD pattern of the nominal BZY electrolyte membrane sintered at 1400 °C for 10 h. (#) YSZ.

would result in a remarkable increase in polarization resistance, and work against attainment of high electrochemical performance.

A single cell with a Ni–BZCY anode and SSC–SDC cathode was used to evaluate the performance of a BZY electrolyte membrane single cell. The cell was tested from 550 to 700 °C with humidified hydrogen (2% H_2O) as the fuel and static air as the oxidant. Fig. 5 shows *I–V* and power density curves of this single cell. The open circuit voltages (OCVs) were 0.953, 0.987, 1.014, and 1.039 V at 700, 650, 600, and 550 °C, respectively. While the maximum power densities were 170, 116, 70, and 41 mW cm^{-2} at 700, 650, 600, and 550 °C, respectively. The OCVs recorded at 600 and 550 °C, were both higher than 1.0 V, which confirmed that the BZY electrolyte membrane was dense enough to prevent gases leakage. This is consistent with the SEM results (Fig. 4). It should be noted that the power performance reported here is the highest to date of cells based on BZY electrolyte [16–18]. Additionally, the performance of the single cell could be further improved by optimizing the microstructure of the anode substrate [19], which would involve adding pore-creating materials or fabricating cells at lower temperatures.

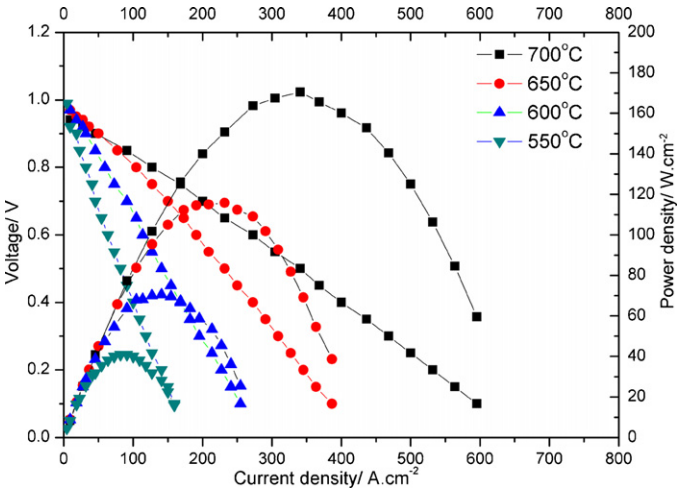

Fig. 5. *I–V* and power density curves of the Ni–BZCY|BZY|SSC–SDC single cell at different temperatures with wet hydrogen (2% H_2O) as the fuel.

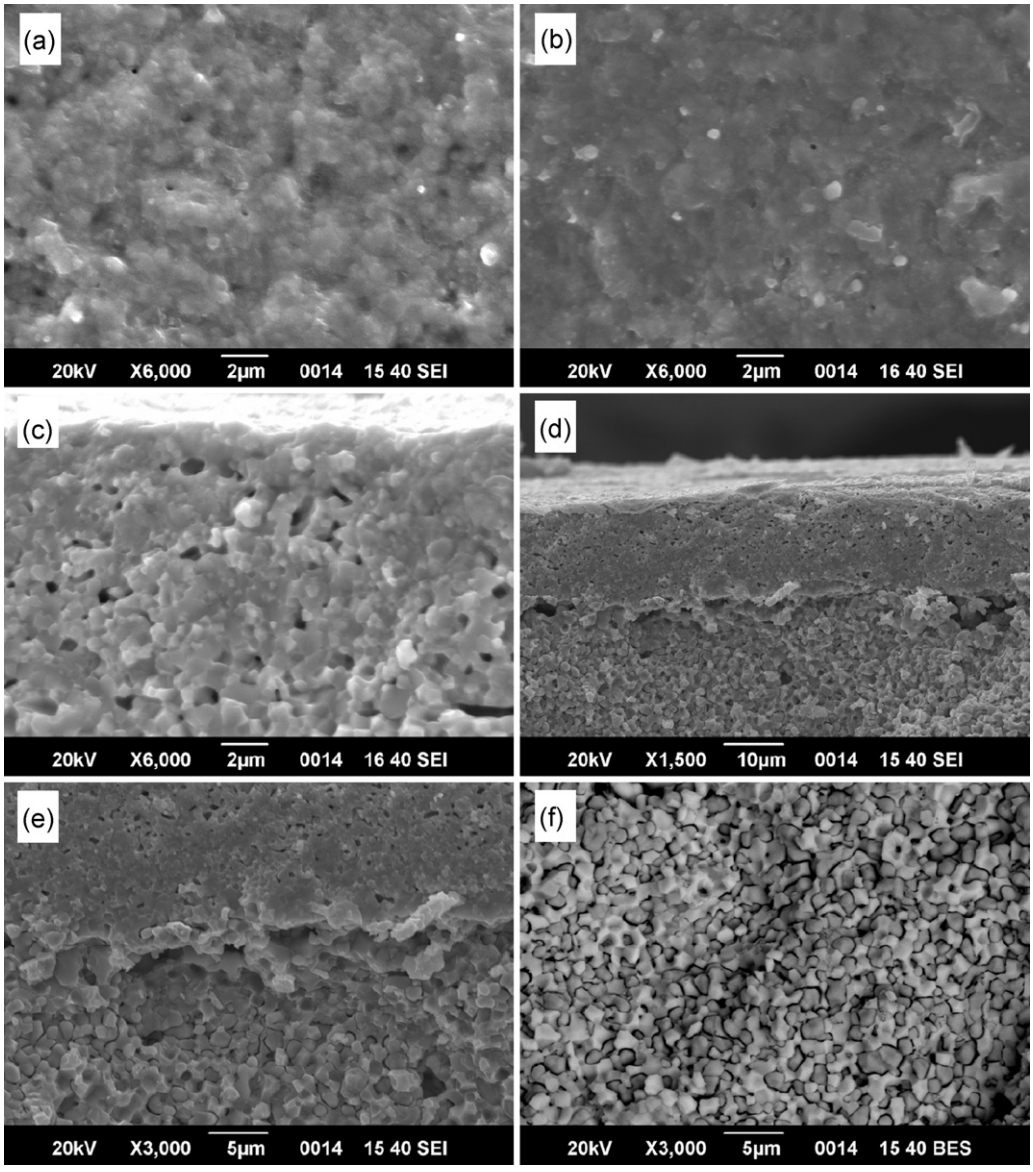

Fig. 4. SEM images of the BZY electrolyte membrane surface morphology before (a) and after (b) testing. SEM images of the cross-section morphologies of the BZY electrolyte membrane after testing (c) and of the tested cell (d–f).

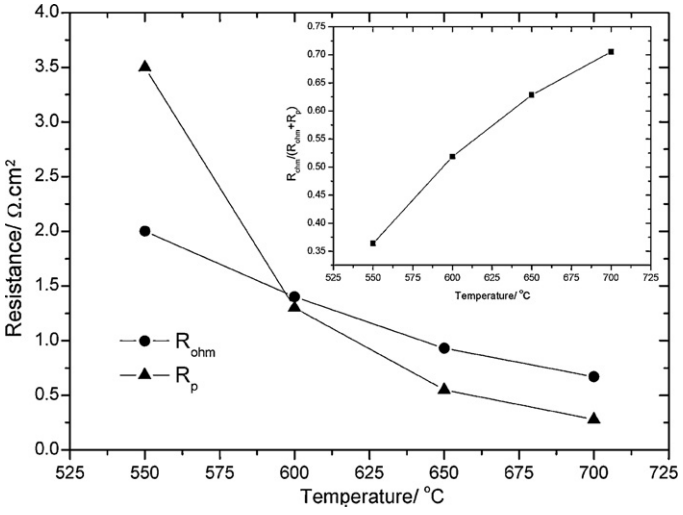

Fig. 6. The ohmic (R_{ohm}) and polarization (R_p) resistances of the tested single cell determined from impedance spectroscopy under open circuit conditions at different temperatures. Inset: the $R_{ohm}/(R_{ohm}+R_p)$ ratio at different temperatures.

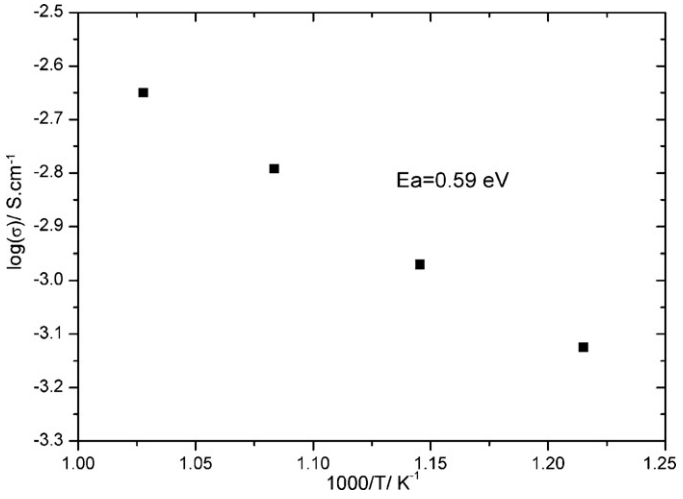

Fig. 7. Conductivity of the BZY electrolyte membrane measured under the cell-testing conditions as a function of temperature.

Fig. 6 shows the ohmic resistances (R_{ohm}) and polarization resistances (R_p) of the tested single cell at different temperatures, and the $R_{ohm}/(R_{ohm}+R_p)$ ratio is insetted in Fig. 6. The resistances were determined from impedance spectroscopy under open circuit conditions. R_{ohm} were 0.67, 0.93, 1.4, and 2.0 $\Omega\,cm^2$, and R_p were 0.28, 0.55, 1.3, and 3.5 $\Omega\,cm^2$ at 700, 650, 600, and 550 °C, respectively. At temperatures higher than 600 °C, R_{ohm} was predominant, accounting for 0.52, 0.63, and 0.71 at 600, 650, and 700 °C, respectively. However, R_p increased much faster than R_{ohm} as the temperature decreased. Consequently, R_p was predominant in the total cell resistance at 550 °C, accounting for about 0.64. It should be noted that the electrode polarization resistances of the cell are far greater than those of other BZCY-based cells using the same SSC–SDC cathode [14]. This is because of the poor anode microstructure (Fig. 4(f)), which is a significant factor restricting the performance of the single cells.

As the electrolyte resistance is predominant in the ohmic resistance under fuel cell conditions, we calculated the conductivity of the BZY membrane (Fig. 7). The BZY membrane showed conductivity of 2.99×10^{-3}, 2.15×10^{-3}, 1.43×10^{-3}, 1.0×10^{-3} S cm^{-1} at 700, 650, 600, and 550 °C, respectively, and the activation energy (E_a) was calculated as 0.59 eV, which is similar to that for $BaZr_{0.8}Y_{0.2}O_{3-\delta}$ pellet sintered at 1600 °C for 8 h [17]. However, compared to $BaZr_{0.8}Y_{0.2}O_{3-\delta}$ pellet, the conductivity of the BZY membrane fabricated at the lower temperature of 1400 °C is much lower, which can be ascribed to its large grain boundary resistance.

4. Conclusions

We successfully used a combined co-press and co-firing process at 1400 °C to fabricate a H-SOFC with a BZY electrolyte membrane supported on a NiO–BZCY anode. The BZY membrane was 20 μm in thick and very dense. A single cell with SSC–SDC as the cathode was tested with wet hydrogen (2% H_2O) as the fuel and static air as the oxidant. The OCVs were 0.953, 0.987, 1.014, and 1.039 V at 700, 650, 600, and 550 °C, respectively. A maximum power density of 170 mW cm^{-2} was obtained at 700 °C. At operating temperatures higher than 600 °C, R_{ohm} was predominant in the total resistance, whereas R_p was predominant at lower temperatures. It is crucial to improve the fabrication technique to obtain higher electrochemical performance for the BZY-based cell.

Acknowledgments

This work was supported by National High-tech R&D Program of China (no. 2007AA05Z157) and Key Program of Chinese Academy of Sciences (no. KJCX1.YW07).

References

[1] H. Iwahara, T. Yajima, T. Hibino, K. Ozaki, H. Suzuki, Solid State Ionics 61 (1993) 65.
[2] H. Iwahara, T. Yajima, H. Ushida, Solid State Ionics 70–71 (1994) 267.
[3] K.H. Ryu, S.M. Haile, Solid State Ionics 125 (1999) 355.
[4] C.D. Zuo, S.W. Zha, M.L. Liu, M. Hatano, M. Uchiyama, Adv. Mater. 18 (2006) 3318.
[5] S.V. Bhide, A.V. Virkar, J. Electrochem. Soc. 146 (1999) 2038.
[6] F.L. Chen, O.T. Sørensen, G.Y. Meng, D.K. Peng, J. Mater. Chem. 7 (1997) 481.
[7] S.W. Tao, J.T.S. Irvine, Adv. Mater. 18 (2006) 1581.
[8] P. Babilo, T. Uda, S.M. Haile, J. Mater. Res. 22 (2007) 1322.
[9] K. Nomura, H. Kageyama, Solid State Ionics 178 (2007) 661.
[10] Y. Yamazaki, P. Babilo, S.M. Haile, Chem. Mater. 20 (20) (2008) 6352.
[11] K.D. Kreuer, Annu. Rev. Mater. Res. 33 (2003) 333.
[12] H.G. Bohn, T. Schober, J. Am. Ceram. Soc. 83 (2000) 768.
[13] K.D. Kreuer, S. Adams, W. Munch, A. Fuchs, U. Klock, J. Maier, Solid State Ionics 145 (2001) 295.
[14] W.P. Sun, L.T. Yan, B. Lin, S.Q. Zhang, W. Liu, J. Power Sources 195 (2010) 3155.
[15] S.W. Tao, J.T.S. Irvine, J. Solid State Chem. 180 (2007) 3493.
[16] C. Peng, J. Melnik, J.X. Li, J.L. Luo, A.R. Sanger, K.T. Chuang, J. Power Sources 190 (2009) 447.
[17] E. Fabbri, D. Pergolesi, A. D'Epifanio, E.D. Bartolomeo, G. Balestrino, S. Licoccia, E. Traversa, Energy Environ. Sci. 1 (2008) 355.
[18] A. D'Epifanio, E. Fabbri, E.D. Bartolomeo, S. Licoccia, E. Traversa, Fuel Cells 1 (2008) 69.
[19] T. Suzuki, Z. Hasan, Y. Funahashi, T. Yamaguchi, Y. Fujishiro, M. Awano, Science 325 (2009) 852.